

Local Quantum Criticality of a One-Dimensional Kondo Insulator Model

W. Zhu^{1,*} and Jian-Xin Zhu^{1,2,†}

¹Theoretical Division, T-4 and CNLS, Los Alamos National Laboratory, Los Alamos, New Mexico 87545, USA

²Center for Integrated Nanotechnologies, Los Alamos National Laboratory, Los Alamos, New Mexico 87545, USA

(Dated: October 27, 2021)

The continuous quantum phase transition and the nature of quantum critical point (QCP) in a modified Kondo lattice model with Ising anisotropic exchange interactions is studied within the density-matrix renormalization group algorithm. We investigate the effect of quantum fluctuations on critical Kondo destruction QCP, by probing static and dynamic properties of the magnetic order and the Kondo effect. In particular, we identify that local Kondo physics itself becomes critical at the magnetic phase transition point, providing unbiased evidences for local quantum criticality between two insulators without resorting to the change of Fermi surface.

Introduction.— Quantum criticality describes the collective fluctuations of matter undergoing a continuous phase transition at zero temperature [1]. As the quantum criticality is central to a broad understanding of strongly correlated quantum matter, how to properly describe the physics around quantum critical points (QCPs) is a subject of intensive research [2]. The intermetallic heavy-fermion compounds [3–5] serve as ideal candidates for the study of quantum phase transition and criticality, by exhibiting unusual properties like heavy-Fermi liquid, magnetic ordering, as well as unconventional superconductivity [6]. Recently, a continuous suppression of antiferromagnetic transition temperature has been discovered in a sizable number of (nearly) stoichiometric heavy fermion systems [2]. For QCPs relevant to the heavy-fermion systems, two major theoretical scenarios have been proposed: One is the spin-density-wave QCP [7, 8] and the other one is critical Kondo destruction QCP [9–11]. For spin-density-wave QCP, conduction electrons acquire peculiar dynamics through an essentially perturbative coupling to the slow critical modes of magnetic background. While in the latter case, the local Kondo physics itself becomes critical at the magnetic ordering transition, and the QCP is driven by the competition between local dynamics and the long-ranged magnetic fluctuations. Despite considerable efforts, debate continues on the nature of QCP, and several issues remain elusive in the heavy-fermion systems. First, it is generally believed that the spin fluctuations in three dimension leads to a Doniach’s QCP [12, 13] with dynamical spin susceptibility satisfying usual Fermi-liquid form, while two-dimensional spin fluctuations tend to favor local QCP with spatially-extended critical degrees of freedom coexisting at the critical point [9]. An important question is what kind of QCP the magnetic transition in one dimension could follow. Second, a key assumption to distinguish different scenarios usually resorts to the shrink of Fermi surface from large to small when across a local QCP [6]. Although the argument of Fermi surface in metallic phase is natural [14–18], the QCP connecting two insulators without Fermi surface is hardly explored, raising the question of whether the change of Fermi surface is intrinsic to the local QCP scenario. Numerically, the extended dynamical mean-field theory (EDMFT) [9, 19–24] and large- N [25, 26] approaches have been used to determine the nature

of QCP in heavy-fermion systems. In these approaches, the spatial and temporal quantum fluctuations are either partially or completely neglected, which is valid in high dimension. Therefore, an unbiased and accurate numerical method to capture the full quantum fluctuations of local moments and itinerant electrons, which become particularly important in low-dimensional systems, is highly desired to clarify the nature of QCP.

The aim of this paper is to address the aforementioned problems, and provide compelling numerical evidences for locally critical phase transition in a microscopic Kondo lattice model (KLM) in one dimension. Based on the density-matrix renormalization group (DMRG) calculations, we are able to access the low-lying energy excitations, static and dynamical correlations of local moments as well as the charge degree of freedom. We first identify a continuous phase transition between Kondo insulator and antiferromagnetic (AFM) phases, signaled by the closing neutral gap and various magnetic order parameters such as magnetization. We then demonstrate the evolution of local susceptibility across the magnetic phase transition. The singular behavior indicates the Kondo screening being critical at the transition point, serving as the hallmark of local quantum criticality. Importantly, we carefully clarify that the conduction electrons form spin density wave, upon the emergence of the AFM order from the local moments. These results provide first compelling evidence of local QCP between two insulators without change of Fermi surfaces.

Model and Method.— We consider a modified Kondo lattice model (KLM) in one dimension with an additional Ising-type interaction between the local spins (Fig. 1), where each unit cell contains a localized spin and an extended conduction-band electron state:

$$H = t \sum_{\langle ij \rangle, \sigma} c_{i\sigma}^\dagger c_{j\sigma} + J_K \sum_i \mathbf{S}_i \cdot \mathbf{s}_i + J_z \sum_{\langle ij \rangle} S_i^z S_j^z. \quad (1)$$

Here $c_{i\sigma}^\dagger$ ($c_{i\sigma}$) denotes the creation operator of a conduction electron with spin $\sigma = \uparrow, \downarrow$ at site i . The \mathbf{S}_i is localized moment with $S = \frac{1}{2}$. Each localized moment interacts via an exchange coupling J_K with the conduction electron, where the conduction electron density is defined as $\mathbf{s}_i = \frac{1}{2} \sum_{\sigma, \sigma'} c_{i\sigma}^\dagger \vec{\sigma}_{\alpha\beta} c_{i\sigma}$. The quantity J_z describes the Ising-

type magnetic exchange interaction between the low moments [38]. We note that the magnetic exchange interaction is usually generated by the Kondo interaction via the Ruderman-Kittel-Kasuya-Yosida (RKKY) effect. Here we have treated it as an independent parameter for two reasons. First, it helps the purpose of specifying the global phase diagram. Second, in one dimension, the Heisenberg-type RKKY interaction always preserves the spin-rotational invariance while the Ising interaction could stabilize AFM order [27]. Therefore, the KLM with Ising-type exchange interaction has the advantage of ameliorating the double counting issue arising from an explicit inclusion of the intrinsic RKKY-based exchange interaction, the latter requiring a treatment of conduction electrons with care [28]. Experimentally, the easy-axis anisotropy widely exists in a number of heavy-fermion systems [29]. Physically, two important mechanisms compete with each other [12, 13]: An isolated local moment would be screened by the spins of conduction electrons through the Kondo screening, while the magnetic exchange interaction tends to induce a long-ranged magnetic ordering. In the absence of Ising-type interaction, the ground state of KLM (at half filling) is spin singlet and the spin gap always exists for any finite exchange J_K , supported by both semiclassical analysis [30] and finite-size numerical calculations [31–34]. In the regime where Ising-type exchange interaction dominates, the AFM phase is expected. Therefore, we expect a magnetic phase transition from the non-magnetic phase to the AFM phase driven by the Ising exchange interaction.

In this work, we study the KLM as described by Eq. (1) using the exact diagonalization (ED) and density-matrix renormalization group (DMRG) method [35]. In DMRG calculations, we use the finite system algorithm with open boundary conditions for system size up to $L = 72$. We use two different $U(1)$ quantum numbers in the DMRG set up. One is the total electron numbers $N^e = n_\uparrow + n_\downarrow$ including number of spin- \uparrow n_\uparrow and spin- \downarrow n_\downarrow electrons, the other one is the z -component

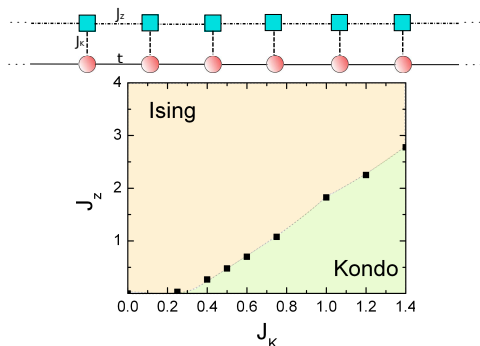


FIG. 1: (Top) One-dimensional Kondo lattice model with an Ising-type interaction between nearest neighbor localized spins. Red dots and blue squares represent the conduction electrons and localized spins, respectively. (Bottom) The global phase diagram as a function of J_z and J_K , by setting $t = 0.25$ (Bandwidth of conduction electron is $4t = 1$). The phase transition is determined to be continuous (see main text).

of pseudo-spin $I^z = (n_\uparrow - n_\downarrow)/2 + S^z$ where S^z is the z -component of the total local moments. To study the Kondo insulator we restrict ourselves to half filling where the total number of conduction electrons N^e equals number of sites L , or the average occupancy is one (half filling). The dynamical response functions are computed within the scheme of dynamical DMRG [36, 37]. By keeping up to 640 states, the truncation error is controlled below $< 10^{-9}$ for static properties and $< 10^{-6}$ for dynamical susceptibility calculations, respectively.

Numerical results.— We first present numerical evidences of Ising anisotropy driven phase transition, based on the low-lying energy spectrum from ED calculation. As shown in Fig 2(a), there exists a doublet ground state manifold in large J_z regime, relating to the AFM ground states in the Ising-limit; while the single ground state in the small J_z regime corresponds to the ground state enclosing spin singlet between a localized spin and one conduction electron state on each lattice site. In particular, upon decreasing J_z , one energy level is continuously gapped out from the ground state manifold, signalling a second-order type phase transition. Here, ED energy spectrum presents the unambiguous evidence of a continuous phase transition from AFM ordered phase to nonmagnetic Kondo insulator phase by tuning down the Ising exchange interaction J_z , whose nature will be addressed by DMRG calculations on the system of large sizes as below.

Further evidences of continuous phase transition can be obtained by DMRG calculations for larger system sizes. Here we define two different energy gaps. First, the energy difference between the ground state and lowest excited state with the same quantum numbers N^e, I^z : $\Delta_N = E_1(N^e = L, I^z = 0) - E_0(N^e = L, I^z = 0)$, is defined as the neutral gap. Second, charge gap is obtained by the energy difference between ground state and lowest excited state with different electron number $\Delta_C = E_0(N^e = L+2, I^z = 0) - E_0(N^e = L, I^z = 0)$. The evolution of energy gaps as a function of J_z is shown in Fig. 2(b). By tuning up J_z , the neutral gap starts to monotonically decrease to zero. In the whole process, the charge gap is always open. The neutral gap continuously goes to zero, supporting a second-order phase transition driven by the Ising anisotropy from the Kondo insulator to an Ising AFM insulat-

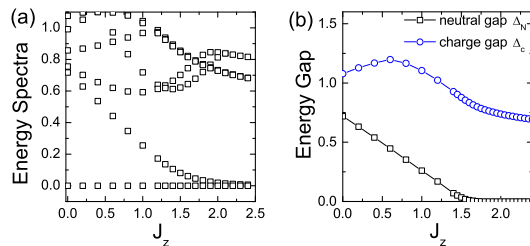


FIG. 2: (a) Energy spectrum evolution as a function of J_z , obtained on $L = 8$ periodic chain by ED calculations. (b) Energy gaps (Δ_N , Δ_C defined in main text) as a function of J_z , obtained on $L = 36$ open chain by DMRG calculations. Here we set $J_K = 1.0$.

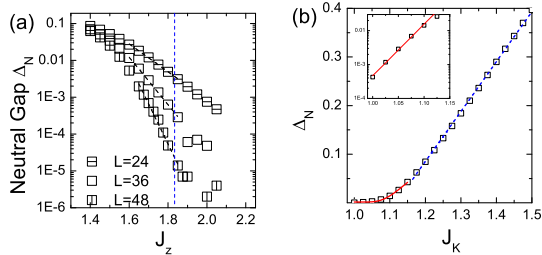


FIG. 3: (a) Log-linear plot of neutral gap Δ_N near the critical point $J_z^c \approx 1.825$, by setting $J_K = 1.0$. Various system sizes are labeled by different symbols. (b) Neutral gap Δ_N as a function of J_K , by setting $J_z = J_z^c = 1.825$. Inset: Log-linear plot of Δ_N and exponential fitting.

ing phase.

It is worth to mention that, the neutral gap shows exponential behavior by approaching the critical point, while away from the critical point the neutral gap is linearly dependent on J_z . As shown in Fig. 3(a), when J_z approaches the critical point, the neutral gap is found to behave as exponentially decayed, for all system sizes. Similarly, by tuning J_K , the neutral gap respectively shows exponential dependence and linear dependence near the critical point and away from the critical point. The exponential dependence of energy scale near the critical point is a signature of the Kondo physics becoming critical.

The phase transition can be described by several local order parameters, as shown in Fig. 4. First, the magnetic order parameter $m_{AF} = \frac{1}{L} \sum_i |\langle S_i^z \rangle|$ develops continuously as J_z exceeds the critical point J_z^c . Importantly, we observe the charge degree of freedom shows the very similar behavior with local moments. Within the numerical uncertainty, the spin density wave pattern ($\Delta n_{SDW} = \frac{1}{L} \sum_i |\langle s_i^z \rangle|$) always occur simultaneously with nonzero magnetization m_{AF} . This excludes the possibility of spin density wave driven phase transition. In addition, magnetic phase transition can also be probed by lattice static susceptibility at magnetic wave vector. The lattice static susceptibility is defined as

$\chi(Q, \omega) = -i \int dt e^{i\omega t} \langle [S_{-Q}^z(t), S_Q^z(0)] \rangle$, where $S_Q^z = \frac{1}{L} \sum_n \sin(\frac{\pi n}{L+1}) S_n^z$ with n being the site index. As shown in Fig. 4, the inverse lattice static susceptibility at magnetic wave vector, $\chi^{-1}(Q = \pi, \omega = 0)$ reaches a minimum at the transition point determined by m_{AF} and Δn_{SDW} . The order parameters, including lattice static susceptibility, magnetization, and charge density imbalance, point to a continuous phase transition between Kondo insulator and the AFM insulator, and determine the magnetic critical point unambiguously.

To uncover the nature of this phase transition, we further investigate the local dynamical response function. For this purpose, we introduce the local spin susceptibility, which is defined as:

$$\chi_{loc}(\omega) = \langle 0 | \Delta S_j^z \frac{1}{\omega - (E_0 - H) + i\eta} \Delta S_j^z | 0 \rangle \quad (2)$$

and $\Delta S_j^z = S_j^z - \langle S_j^z \rangle$ (we choose site j in the center of the chain). Figure 5 shows the local spin susceptibility around the quantum critical point. In the Kondo singlet phase $J_z < J_z^c$, the peak of $\Im \chi_{loc}(\omega)$ stands away from the zero frequency. This peak position as a measure of the gapped spin excitations has a one-to-one correspondence to the value of the neutral gap as shown in Fig. 2(b). As J_z increases, the dominate peak moves towards the low frequency, and reach zero frequency around $J_z \approx J_z^c$. Near the critical point J_z^c , $\Im \chi_{loc}(\omega = 0)$ becomes steeper, which leads to a peak structure developing at $\Re \chi_{loc}(\omega = 0)$. The J_z value at which $\Re \chi_{loc}(\omega = 0)$ reaches the maximum defines the critical point J_z^c . Since the singular behavior $\Re \chi_{loc}(\omega)$ around zero-frequency is key to the nature of QCP, we inspect the $\Re \chi(\omega)$ in detail in Fig. 6. We show the semi-logarithmic plot of $\Re \chi_{loc}(\omega)$ with a focus on low-frequency regime. It is found that, for the Kondo insulator phase $J_z < J_z^c$, $\Re \chi_{loc}(\omega \rightarrow 0)$ saturates to a finite value in the low-frequency limit (Fig. 6(b)), however, around the critical point $J_z \approx J_z^c$, $\Re \chi_{loc}(\omega \rightarrow 0)$ shows distinct behavior. To demonstrate the singular behavior of $\Re \chi_{loc}(\omega = 0)$, we investigate the $\Re \chi_{loc}(\omega = 0)$ dependence on η , which is imaginary part in dynamical response function Eq. (2). To the best fit, we determine that the inverse of $\Re \chi_{loc}(\omega = 0)$ has a

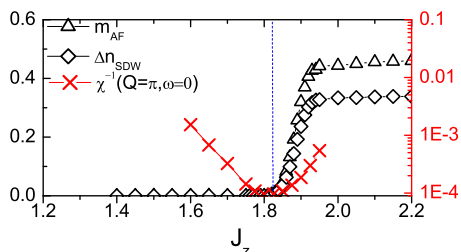


FIG. 4: Antiferromagnetic order parameter $m_{AF} = \frac{1}{L} \sum_i |\langle S_i^z \rangle|$ (black triangular) and spin density wave order parameter $\Delta n_{SDW} = \frac{1}{L} \sum_i |\langle s_i^z \rangle|$ (black diamond), and inverse static spin susceptibility $1/\chi(Q = \pi, \omega = 0)$ (red cross) as a function of J_z . Blue dashed line marks the transition point $J_z^c \approx 1.825$.

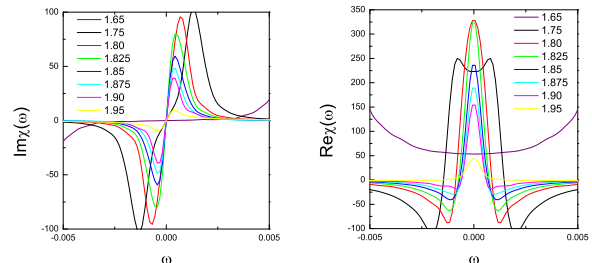


FIG. 5: Frequency dependence of the local spin susceptibility at various values of J_z around the magnetic transition: (Left panel) Imaginary part and (Right panel) Real part. Here we choose $J_K = 1.0$.

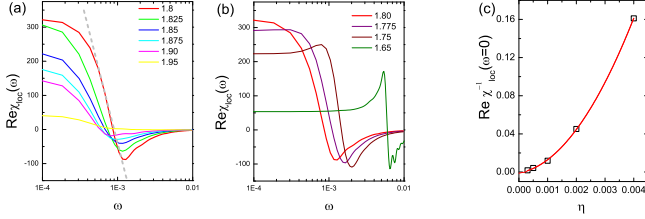


FIG. 6: Semi-log plot of the real part of the local spin susceptibility around the magnetic transition: (a) $J_z > J_z^c$ and (b) $J_z < J_z^c$. (c) Inverse of the real part of the local spin susceptibility $\Re\chi_{loc}^{-1}(\omega=0)$ versus η . Red line shows the polynomial function fitting: $\Re\chi_{loc}^{-1}(\omega=0) = A\eta^2 + B\eta + C$, with nonzero A , B and $C = -0.0013 \pm 0.002$.

polynomial dependence on η (Fig. 6(c)). In the intrinsic limit ($\eta \rightarrow 0$), we determine that $\Re\chi_{loc}^{-1}(\omega=0)$ is scaled to zero within the fitting accuracy, thus $\Re\chi_{loc}(\omega=0)$ becomes singular. Physically, the divergence of local susceptibility signals the Kondo screening being critical, which is the hallmark of local quantum criticality [6, 9]. Here we emphasize that, compared with previous studies [22–24], the advantage of current scheme is that we can target the behavior at zero frequency $\Re\chi_{loc}(\omega=0)$ directly, instead of relying on extracting the scaling behavior first in the low frequency. An additional support for critical local physics is provided by a logarithmically scaling form [9]: $\Re\chi_{loc}(\omega) \sim \alpha \ln|\omega|^{-1}$ within energy window $T_K^* < \omega < T_K^0$, where the effective Kondo scale T_K^* vanishes logarithmically slowly as approaching critical point $J_z \rightarrow J_z^c$. In Fig. 6(a), we show such kind of scaling behavior indeed emerges in the vicinity of zero frequency (gray dashed line).

One more advantage of our method is to treat the spin and charge degrees of freedom on an equal footing. Here we show the electron spectrum density, $\rho_\sigma(\omega) = \frac{1}{L} \sum_i \rho_{i\sigma}(\omega)$, around the phase transition in Fig. 7(a), where $\rho_{i\sigma}(\omega) = -\frac{1}{\pi} \Im \langle 0 | c_{i\sigma} \frac{1}{\omega - (E_0 - \hat{H}) + i\eta} c_{i\sigma}^\dagger | 0 \rangle$. In the Kondo insulator phase ($J_z = 1.65 < J_z^c$), the electron density is uniformly distributed in real space, and the spectrum density is gapped

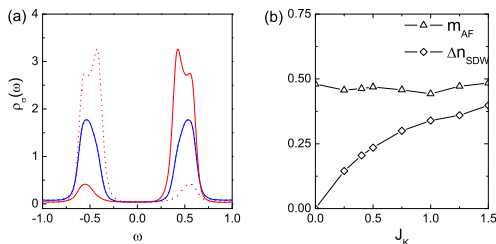


FIG. 7: (a) Local electron spectrum density as a function of ω for $J_z = 1.65$ (blue) and $J_z = 1.95$ (red). Solid and dotted line represents spin-down and spin-up component, respectively. (b) In the Ising AFM phase, the J_K dependence of magnetization m_{AF} and charge polarization Δn_{SDW} .

with equal weight below and above the Fermi energy. In the AFM phase ($J_z = 1.95 > J_z^c$), the spin-density wave pattern is formed in real space, which results in an imbalance of the spectral weight of the spin-resolved spectral density in the lower and upper gap edges. In particular, the gap around the Fermi energy in the spectrum density remains open as J_z crosses the critical point, consistent with the charge gap evolution in Fig. 2(b). This result is in striking contrast to the expectation from the Gutzwiller variational wavefunction or other auxiliary mean-field methods [39–41] even for the one-dimensional systems that the quasiparticle gap in the conduction electron sector should be closed at the critical point. In addition, we find that, in the Ising AFM phase the magnitude of spin polarization Δn_{SDW} strongly depends on J_K , while the local moment magnetization m_{AF} is almost unchanged. These facts indicate that the spin-density wave in the conduction electron sector is “slave” to the local spin AFM order, partially supporting the local critical picture.

Conclusion.— We have presented a thorough numerical study of a continuous phase transition between the Kondo insulator and the antiferromagnetic phases in a modified Kondo lattice model, which is of great present interest in connection with heavy-fermion quantum criticality. Around the magnetic phase transition point, the magnetic order parameter vanishes continuously and the static susceptibility at the magnetic ordering wave vector diverges. A concomitant divergence of the static local susceptibility signals that the Kondo physics also becomes critical at the quantum critical point. These results provide a “proof-of-the-principle” example that the local quantum criticality [9] can also occur for the transition between two insulating phases, where the Fermi surface becomes irrelevant. It indicates that the local quantum criticality is a paradigm for novel phase transitions, which deserves to be explored in other areas of physics (e.g., the interplay between strong correlation and topology in heavy fermion systems).

Acknowledgments.— This work was supported by U.S. DOE at Los Alamos National Laboratory under Contract No. DE-AC52-06NA25396 through the LANL LDRD Program (W.Z.), and U.S. DOE Office of Basic Energy Sciences (J.-X.Z.). It was supported in part by the Center for Integrated Nanotechnologies, a U.S. DOE Basic Energy Sciences user facility.

* Electronic address: weizhu@lanl.gov

† Electronic address: jxzh@lanl.gov

- [1] S. Sachdev, *Quantum Phase Transitions* (Cambridge University Press, Cambridge, 2nd Ed., 2011).
- [2] H. v. Lohneysen, A. Rosch, M. Vojta, and P. Wolfle, *Rev. Mod. Phys.* **79**, 1015 (2007).
- [3] G. R. Stewart, *Rev. Mod. Phys.* **56**, 755 (1984).
- [4] H. Tsunetsugu, M. Sigrist, and K. Ueda, *Rev. Mod. Phys.* **69**, 809 (1997).
- [5] G. R. Stewart, *Rev. Mod. Phys.* **73**, 797 (2001); **78**, 743 (2006).
- [6] P. Genenwart, Q. M. Si, and F. Steglich, *Nat. Phys.* **4**, 186

- (2008).
- [7] J. A. Hertz, Phys. Rev. B **14**, 1165 (1976).
- [8] A. J. Millis, Phys. Rev. B **48**, 7183 (1993).
- [9] Q. Si, S. Rabello, K. Ingersent, and J. L. Smith, Nature **413**, 804 (2001).
- [10] T. Senthil, S. Sachdev, and M. Vojta, Phys. Rev. Lett. **90**, 216403 (2003).
- [11] P. Coleman and A. H. Nevidomskyy, J. Low Temp. Phys. **161**, 182 (2010).
- [12] S. Doniach, Physica B **91**, 231 (1977).
- [13] C. M. Varma, Rev. Mod. Phys. **48**, 219 (1976).
- [14] J. C. Xavier, E. Novais, and E. Miranda, Phys. Rev. B **65**, 214406 (2002).
- [15] S. A. Basylko, P. H. Lundow, and A. Rosengren, Phys. Rev. B **77**, 073103 (2008).
- [16] M. Troyer and D. Wurtz, Phys. Rev. B **47**, 2886 (1993).
- [17] H. Tsunetsugu, M. Sgrist, and K. Ueda, Phys. Rev. B **47**, 8345R (1993).
- [18] S. Moukouri and L. G. Caron, Phys. Rev. B **54**, 12212 (1996).
- [19] D. R. Grempel and Q. Si, Phys. Rev. Lett. **91**, 026401 (2003).
- [20] J.-X. Zhu, D. R. Grempel, and Q. Si, Phys. Rev. Lett. **91**, 156404 (2003).
- [21] P. Sun and G. Lotliar, Phys. Rev. Lett. **91**, 037209 (2003).
- [22] J.-X. Zhu, S. Kirchner, R. Bulla, and Q. Si, Phys. Rev. Lett. **99**, 227204 (2007).
- [23] M. T. Glossop and K. Ingersent, Phys. Rev. Lett. **99**, 227203 (2007).
- [24] M. T. Glossop and K. Ingersent, Phys. Rev. B **75**, 104410 (2007).
- [25] I. Paul, C. Pépin and M. R. Norman, Phys. Rev. Lett. **98**, 026402 (2007).
- [26] C. Pépin, Phys. Rev. Lett. **98**, 206401 (2007).
- [27] N. Ishimura and H. Shiba, Prog. Theor. Phys. **63**, 743 (1980).
- [28] Q. Si, J.-X. Zhu, and D. R. Grempel, J. Phys.: Condens. Matter **17**, R1025 (2005).
- [29] H. Tsujii *et al.*, Phys. Rev. Lett. **84**, 5407 (2000).
- [30] A. M. Tsvelik, Phys. Rev. Lett. **72**, 1048 (1994).
- [31] H. Tsunetsugu, Y. Hatsugai, K. Ueda, and M. Sgrist, Phys. Rev. B **46**, 3175 (1992).
- [32] C. C. Yu and S. White, Phys. Rev. Lett. **71**, 3866 (1993).
- [33] N. Shibata, T. Nishino, K. Ueda, and C. Ishii, Phys. Rev. B **53**, 8828(R) (1996).
- [34] N. Shibata and K. Ueda, J. Phys.: Condens. Matter **11**, R1 (1999).
- [35] S. R. White, Phys. Rev. Lett. **69**, 2863 (1992).
- [36] T. Kuhner and S. White, Phys. Rev. B **60**, 335 (1999).
- [37] E. Jeckelmann, Phys. Rev. B **66**, 045114 (2002).
- [38] Compared to the Hamiltonian defined in previous works [19, 20], the Ising exchange term in Eq. (1) has a factor 1/2 difference.
- [39] J.-X. Zhu, J.-P. Julien, Y. Dubi, and A. V. Balatsky, Phys. Rev. Lett. **108**, 186401 (2012).
- [40] J.-X. Zhu, I. Martin, and A. R. Bishop, Phys. Rev. Lett. **100**, 236403 (2008).
- [41] T. Senthil, M. Vojta, and S. Sachdev, Phys. Rev. B **69**, 035111 (2004).